# A theoretical model to predict interface slip

O. T. Tsioulou

Civil Engineer, MSc

S. E. Dritsos

Professor, RILEM senior member

*Department of Civil Engineering, University of Patras, 26500, Patras, Greece.*

Tel: 00302610-997780

Fax: 00302610-996575

e-mail address: dritsos@upatras.gr

URL: http://www.episkeves.civil.upatras.gr/

**Abstract** Casting a new concrete layer on the tensile or compressive side of a reinforced concrete element is a common technique that is used to increase the flexural capacity of weak reinforced concrete elements. Until now however, a model has not been presented in the literature to evaluate the slip between the two components. Usually, in common practical design, slip is ignored and the strengthened element is assumed monolithic. This may not be a conservative assumption, as any slip would affect the ultimate resistance of the strengthened element. In the present paper, an analytical procedure is presented that predicts the distribution of slip strain, slip and shear stress along a reinforced or unreinforced interface between an initial beam and a new concrete layer. By following this process, the capacity of a strengthened beam is determined by taken slip into account. In addition, a step-by-step design procedure is presented and then applied to an experimental result. Good agreement if found. Further verification of the analytical procedure is performed by comparison with finite element analysis and very good agreement is found.

***Keywords*** *strengthening; concrete beams; concrete layers; interface; shear stress; slip strain; slip.*

# 1. Introduction

The addition of a new concrete layer on the compressive or tensile side of an element is a technique that is used to strengthen concrete elements that are weak in flexure. This practice has been the object of many experimental investigations (Altun 2004; Banta 2005; Bass et al. 1985; Cheong and MacAlevey 2000; Dimitriadou et al. 2005; Dritsos 1994; Hanson 1960; Loov and Patnaik 1994; Mast 1968; Mattock 1976; Pauley et al. 1974; Saemann and Washa 1964; Silfwerbrand 1990; Silfwerbrand 2003; Tassios 1983; Trikha et al. 1991; Vassiliou 1975; Vintzeleou 1984; Vrontinos et al. 1989; Zervos and Beldekas 1995). Usually, in design, it is assumed that full interaction between old and new components exists across the interface. However, in reality, slip and in some cases separation at the interface cannot be prevented. Therefore, since the amplitude of slip at the interface may affect the stiffness and the ultimate resistance of a strengthened element, it may be necessary to consider it.

In design, to simplify calculations, it is usual to consider monolithic behaviour of the concrete composite element and, in order to take into account the interface slip effect, the use of appropriate correction factors has been proposed in the literature (Dritsos 1996; Dritsos 2007; Thermou et al. 2007) to correct parameters or results obtained under the monolithic behaviour assumption. This design practice has been adopted in recent design codes (CEN 2005, GRECO 2009). Clearly, the amplitude of the interface slip directly affects the above correction factor values (Dritsos 1996; Dritsos 2007; Thermou et al. 2007).

It is worth noting that slip along a joint is directly correlated with respective crack openings (CEB-FIP 2008; CEB-FIP Model Code 90 1993; Vintzileou 1986; Tsoukantas and Tassios 1989) and affects the level of damage to a strengthened element. Therefore, interface slip is a critical parameter that should be assessed when the fulfillment of specific acceptance criteria for a desired damage or performance level of the strengthened element is to be examined.

Obviously, if a composite concrete element has to remain practically free of damage, small slip values can be accepted. On the other hand, if the limit state of significant damage or the performance level of life protection or failure prevention is desired, rather higher interface slip values are usually accepted. It should be stated that in recent design codes (FEMA 2000; GRECO 2009), specific limit values for interface slip or crack openings are adopted with respect to desired performance or damage levels. For example, according to the Greek Retrofitting Code (GRECO 2009), the maximum accepted value of interfacial slip for level A (corresponded to the immediate occupancy performance level or the damage limitation limit state) is 0.2 mm, for level B (corresponded to the life safety performance level or the significant damage limit state) it is 0.8 mm and for level C (corresponded to the collapse prevention performance level or the near collapse limit state) it is 1.5 mm. Alternatively, in FEMA (FEMA 2000), maximum crack opening values should not exceed 1.6 mm or 3.2 mm for immediate occupancy and life safety respectively.

Finally, the amplitude of interface slip is important as far as durability is considered, since it affects the transmission of water or de-icing salts along the interface.

Obviously, in some design cases, the assessment of the interface slip amplitude is necessary. The aim of this study is to model the interface slip effect and to propose an analytical procedure to evaluate the slip distribution of concrete

composite elements subjected to bending. Subsequently, the corresponding flexural capacity of the composite element can be determined.

## 2. Strengthening using concrete layers

By adding a new concrete layer to an original beam, a concrete-to-concrete composite element is created. The flexural behaviour of this composite element depends on the connection between the old and the new components. There are a number of shear load transfer models in the literature that simulate the condition of the connection at the interface. Most of these models (CEB-FIP 2008; GRECO 2009; Tassios 1983; Vintzeleou 1984) give a relationship between the shear stress and the slip at the interface between the two components, while others give a relationship between the shear stress and the slip strain (Dritsos 1994; Dritsos and Pilakoutas 1995; Kotsira et al. 1993; Saidi et al. 1990). Fig. 1 presents strain distribution profiles of a strengthened beam for different connection conditions between the two different concrete components. If the connection is perfect, there is no slip at the interface between the new and the old concrete and the composite element behaves as if monolithic. In this case, when the composite beam is loaded and bends, the strain distribution profile is continuous, as shown in Fig. 1a. If there is no connection at the interface, the old and the new concrete behave independently during loading and the strain distribution for this case is shown in Fig. 1b. In most cases, there is a partial connection between the old and the new concrete. Obviously, the slip between the two components depends on the shear stress activated at the interface. In this situation, three main possible strain distribution profiles can be recognized, as shown in Figs. 1c, 1d and 1e, depending on the magnitude of the interface slip strain and the relevant position of the interface in relation to the height of the bent section. The first type of strain distribution occurs when the interface lies in the tensile zone of the composite element, as shown in Fig. 1c. When the interface lies in the compression zone, the strain distribution is as shown in Fig. 1d. Fig. 1e presents the last type of strain distribution, which usually occurs when there are high values of slip at the interface resulting in tensile and compressive zones on either side of the interface.

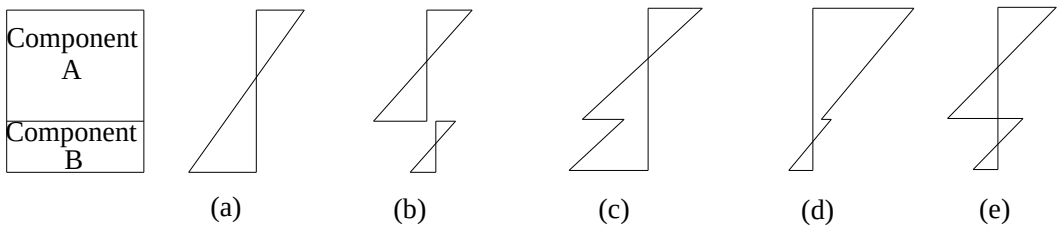


**Fig. 1** - Strain distribution profiles of a loaded strengthened composite beam for different interface connection conditions a) perfect connection, b) no connection c), d) and e) partial connections

Apart from slip due to bending the composite element, there is also slip due to the new concrete layer shrinking after being placing. The substrate concrete restrains this additional shrinkage and values of the concrete strain at the interface are less than free shrinkage strain. Furthermore, there is an extra reduction of slip due to creep. These two mechanisms had been analysed and investigated and can be found in the literature (ACI 1971; Beushausen and Alexander 2006; Beushausen and Alexander 2007; Birkeland 1960; Silfwerbrand 1997; Yuan and Marsszeky 1994; Yuan et al. 2003). Usually, this extra slip due to shrinkage and creep is low when compared to the slip due to bending and it could be ignored (Lampropoulos

and Dritsos 2008). Nevertheless, in the literature (Beushausen and Alexander 2007; Birkeland 1960; Silfwerbrand 1997; Yuan et al. 2003; Yuan and Marsszeky 1994; Zhou et al. 2008), there are analytical procedures to evaluate the effect of shrinkage stresses that may act on the new concrete layer.

# 3. Shear force transfer mechanisms at the new-old concrete interface

When a concrete element is strengthened by a new concrete layer, three mechanisms contribute to the shear resistance at the interface. These are concrete to concrete adhesion, concrete to concrete friction and the connecting action from steel bars placed across the interface between the old and the new concrete. These three mechanisms can be subdivided into the two groups of unreinforced and reinforced interfaces, depending on whether or not additional steel is placed across the interface of the old and new concrete.

In the case of unreinforced interfaces, the two mechanisms acting at them are adhesion and friction. It must be noted that maximum adhesion values are achieved for low interface slip values, while friction becomes important for much higher values of slip. Therefore, the maximum resistances from adhesion and friction cannot be consider to act together.

In the case of reinforced concrete interfaces, when the interface between the old and the new concrete is roughened or when shotcrete has been placed and the steel bars at the interface are well anchored, clamping action may occur. When a shear stress is applied, a slip is produced and the contact surface between the old and the new concrete must open as one surface rides up the other due to the roughness. Therefore, a tensile stress is activated in the steel bar, which in turn produces a corresponding compressive stress, or clamping action, and a frictional resistance is mobilised. Furthermore, the slip at the interface, deform the interface steel bars which in turn compress the concrete. Because of equilibrium, concrete causes forces opposite to the interface slip activating the dowel action.

Analytical $\tau$ against $s$ models, concerning each possible interface mechanism, have been proposed in the literature (CEB Bulletin No 162 1983; CEB-FIP 2008; Tassios 1983; Vintzeleou 1984) and similar expressions have been adopted in design codes (CEB-FIP 1993; GRECO 2009) in the form presented in Fig. 2.

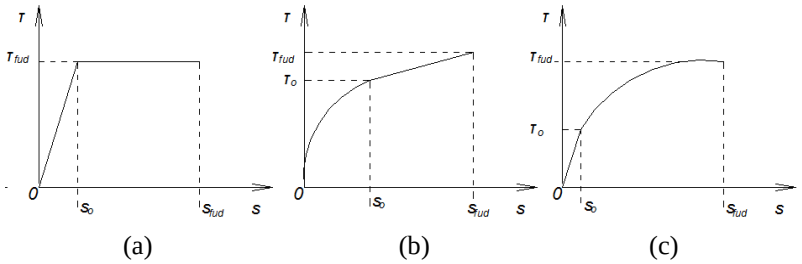


(a) (b) (c)

**Fig. 2** - Theoretical τ against s models for a) adhesion, unreinforced interface and friction, unreinforced smooth interface, b) friction, unreinforced rough interface and c) reinforced interface

In Fig. 2, $\tau_{fud}$ is the ultimate interface shear strength, $s_{fud}$ is the maximum slip, $\tau_o$ is the shear stress at the point where there is a change in the $\tau$ against $s$ curve and $s_o$ is the respective value of slip for shear stress $\tau_o$.

Values for coefficients $s_o$, $\tau_o$, $s_{fud}$ and $\tau_{fud}$ and respective equations for the theoretical models shown in Fig. 2 can be found in the literature (CEB Bulletin

No 162 1983; CEB-FIP 1993; CEB-FIP 2008; GRECO 2009; Tassios 1983; Vintzeleou 1984).
In reality, the total shear resistance between contact surfaces can be found by ssuming the individual shear resistances that are mobilised by each individual mechanism for a common interface slip. Fig. 3 presents a plot of the superposition of slip from all the mechanisms discussed above for the transfer of shear stress at the interface.
As it can be seen from Fig. 3, the problem becomes complicated when all the mechanisms are considered to act together. When considering the required performance level, if an acceptable value of slip is determined, the respective interface resistance can be found by calculating the resistance for each mechanism and summing the results.
For very low values of slip, only the mechanism of adhesion is activated. After adhesion is destroyed, the other two mechanisms, friction and dowel action, are taking place. Therefore, a general interface model could be adopted by superposing the above individual models, as in Eqs. (1) and (1a).

$$\tau_x = f(s_x) \tag{1}$$

where $f(s_x)$ is a polynomial function. In the case that accurate results are required, specific experiment, proper for the case which is examined, are required. Otherwise, approximately, a combination of the theoretical models given in literature (CEB Bulletin No 162 1983; CEB-FIP 1993; CEB-FIP 2008; GRECO 2009; Tassios 1983; Vintzeleou 1984), can be used.
In general, it can be considered:

$$f(s_x) = k_s \cdot s_x \tag{1a}$$

For low $s_x$ values $0 \le s_x \le s_1$, a linear relationship can be adopted (Fig. 3):

$$f(s_x) = k_{s,o} \cdot s_x \tag{1b}$$

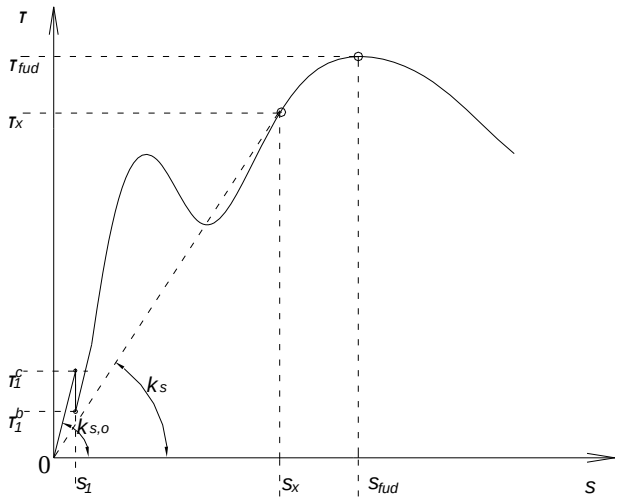


**Fig. 3** - Combined mechanism $\tau$ against $s$ model for a concrete interface

In Fig. 3, $\tau_x$ and $s_x$ are the shear stress and respective slip at section $x$, $s_1$ is the slip at adhesion failure, $\tau_1^c$ and $\tau_1^b$ are respectfully the maximum and minimum interface shear strength resistances before and after adhesion failure, $k_{s,o}$ is a

coefficient expressing the initial stiffness for $s < s_1$, $k_s$ is the target stiffness for $s = s_x$.

Except for the analytical shear stress – slip curves presented above, existing design codes (ACI Committee 318 2004; BS 8110-1 1995; CEN 2004; CSA A23.3 1994; PCI 1992; SABS 0100-1 1992) suggest analytical equations in order to calculate the shear strength at the interface and there are also some analytical models presented in the literature (Birkeland and Birkeland 1966; CEB-FIP 2008; Loov and Patnaik 1994; Mast 1968; Mattock 1976; Saemann and Washa 1964; Shaikh 1978) in order to calculate the shear strength at the interface.

All the above are about theoretical models for the shear transfer at the interface. In literature, a number of experimental test results have been presented (Banta 2005; Dimitriadou et al. 2005; Dritsos et al. 1996; Hanson 1960; Loov and Patnaik 1994; Mattock 1976; Pauley et al. 1974; Saemann and Washa 1964; Vassiliou 1975; Vintzeleu 1984) in the form of shear stress against slip diagrams for concrete interfaces. A summary of the these results are presented in Fig. 4 in terms of the interface shear stress ($\tau$), normalized by the average tensile strength ($f_{cm}$) of the weakest concrete, against the slip ($s$). The experimental set up, concrete strength, type of interface and dimensions of the interface are some of the parameters involved in these tests. Three main groups of experimental results can be recognised with regard to the interface type and the mobilized shear mechanism. Fig. 4a presents the first group, which represents experimental results for unreinforced smooth and rough concrete interfaces without normal to the interface stresses. In this situation, adhesion could be considered as the main mobilized interface shear resistance. Adhesion is the shear resistance of the interface in the absence of both a compressive force normal to the interface and of clamping reinforcement crossing it. It is mainly due to chemical connection of the new concrete to the existing one (CEN 1998). Adhesion is influenced by the roughness and the treatment of joint surface (CEB Bulletin No 162 1983) and as a result, interface interlock is concluded in this definition. Fig. 2b presents the second group, which show experimental results for unreinforced smooth and rough concrete interfaces with a normal to the interface stress of 0.5 MPa (Vas.1, Vintz.1, Vas.3, Vintz.3) or a normal to the interface stress of 2.0 MPa (Vas.2, Vintz.2, Vas.4, Vintz.4). In case of unreinforced concrete interface with normal to the interface stress, the shear resistance is made up by both friction and adhesion. In both above experimental works (Vintzileou 1984, Vassiliou 1975), there is no adhesion at the interface. In Vintzeleou's (1984) work, the experiments were taken place after a crack was made in the specimen and in Vassiliou's (1975) experiments, the two prisms were casted separately and then they were put in contact in order to create the composite specimen. In this case, friction could be considered as the mobilized interface shear resistance. Finally, Fig. 4c presents the third group, which are experimental results for reinforced smooth and rough concrete interfaces without normal to the interface stresses. A push-off test set up was used in most of the experiments shown in Figs. 4a, 4b and 4c. Fig. 5a schematically presents some common push-off test arrangements (Hanson 1960, Vassiliou 1975, Banta 2005), while some other researchers (Vintzileou 1984, Dritsos et al. 1996, Dimitriadou et al. 2005, Mattock 1976) used the arrangement shown in Fig. 5b. Briefly, new concrete is cast against a previously prepared surface or surfaces of old concrete and the arrangement is loaded in the presence or not of normal to the interface stress. Alternatively, results from Saemann and Washa (SW) (Saemann and Washa 1964), Loov and Patnaik (LP) (Loov and Patnaik 1994) and some from Hanson (Hg) (Hanson

1960) concern concrete beams strengthened with concrete layers. These results for concrete beams strengthened with concrete layers are depicted in Fig. 4d, for different types of surfaces. Figs 4a-4c show the results of push-off tests in the type of one shown in Fig. 5. For the case that the only interface mechanism is adhesion, the push-off test results shown in Fig. 4a, concern only maximum values of $\tau$ and $s$ while, for beams shown in Fig. 4d, the whole interface behaviour is represented by $\tau$ against $s$ curves.

It can be seen from Fig. 4 that, depending on the parameters involved, there are a wide range of results. In several cases, maximum values are obtained for very low values of slip. Obviously, rough interfaces are better than smooth interfaces. It also can be seen that at reinforced interfaces, maximum value of shear stress is greater that in unreinforced interfaces. Although experimental results depicted in Fig. 4b, are for unreinforced interfaces with normal stress, the maximum values of shear stress are almost in the same range as in the case of unreinforced interfaces without normal to the interface stress which is presented in Fig. 4a. This happens because, as it has already been reported, in both experimental works of Vintzileou (1984) and Vassiliou (1975), there is no adhesion at the interface

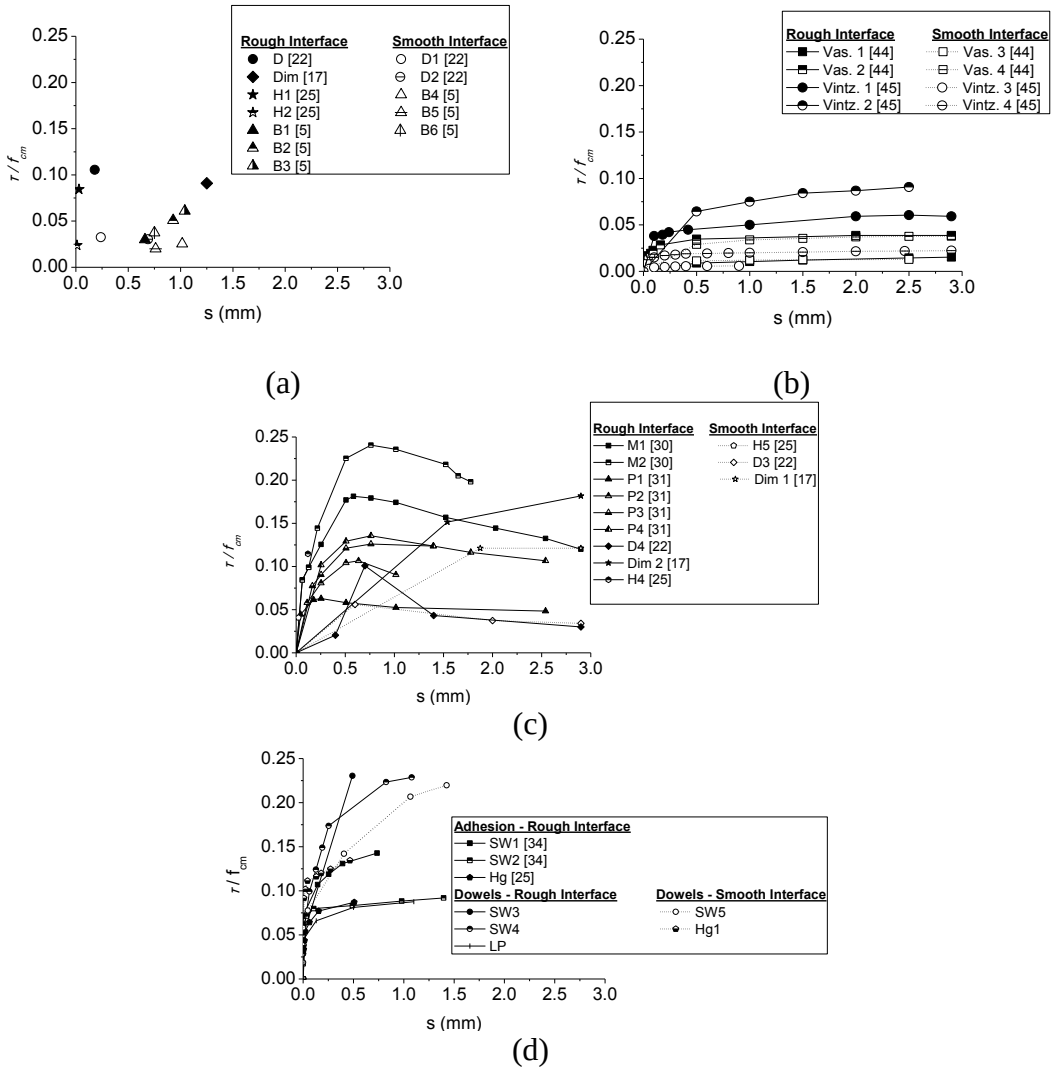


**Fig. 4** - Experimental $\tau/f_{cm}$ against slip curves from push-off tests for a) unreinforced interfaces without normal to the interface stress (adhesion), b) unreinforced interfaces with normal to the interface stress (friction), c) reinforced interfaces without normal to the interface stress and d) experimental $\tau/f_{cm}$ against slip curves for concrete beams strengthened with concrete layers

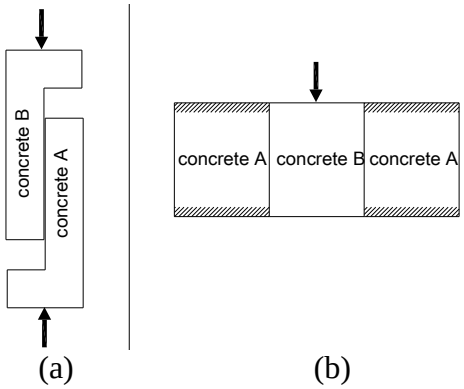


**Fig. 5** - Common push-off test arrangements a) Hanson 1960, Vassiliou 1975, Banta 2005 and b) Vintzileou 1984, Dritsos et al. 1996, Dimitriadou et al. 2005, Mattock 1976

By considering all the experimental results of Fig. 4 above, it can be deduced that values for $k_s$ range from 0.5 MPa/mm to 95 MPa/mm. In every case, a $\tau$ - $s$ experimental curve, from a specific experiment, should be chosen. Otherwise, a theoretical and as a result, not so accurate, $\tau - s$ curve proposed in literature (CEB Bulletin No 162 1983; CEB-FIP 1993; CEB-FIP 2008; GRECO 2009; Tassios 1983; Vintzeleou 1984), should be chosen.

# 4. Assumptions

The determination of the slip distribution along the interface due to bending a strengthened composite element is complicated. In order to simplify the problem, the following assumptions have been made:
During bending, plane sections of each element remain plane (Navier-Bernoulli's assumption),
The bond between the reinforcement and the concrete is perfect, so no slip between longitudinal reinforcement and concrete is assumed,
The relationship between concrete compressive stress and strain is assumed to be parabolic-rectangular adopting the EC2 concrete model (CEN 2004) with an ultimate strain of -0.0035 and the maximum acceptable compressive stress is $0.85f_c$, (where $f_c$ is the concrete compressive strength),
The stress against strain relationship of the steel is assumed elastoplastic with a modulus of elasticity ($E_s$) of 200 GPa.
The depth of a bonding layer, if existing, is assumed zero. This means that even there is a bonding layer, as for instance a layer of resin, the layer thickness is assumed zero and it is taken into account through specific interface conditions.
The composite element is considered to fail when the top fibre of the upper element reaches the ultimate strain (-0.0035),
The composite element is consider to yield when the strain of the upper or the lower component steel reaches its yield value ($\varepsilon_{sy} = f_y/E_s$, where $f_y$ is the yield stress of the steel) and
The curvature of the beam and the additional layer is the same at any section through the strengthened beam and, therefore, only longitudinal separation is considered.
A more analytical explanation of these assumptions is presented in the following section. Shrinkage stresses are ignored and the relationship between the shear stress and the bending slip is assumed to be given by Eq. (1) above. In order to give reliable results, coefficient $k_s$ must take reliable values.

# 5. Analytical evaluation of bending slip along the interface of a strengthened beam

Consider a concrete beam strengthened by the addition of a new concrete layer. Fig. 6 presents a part of the loaded beam and the respective bending moment diagram. In Fig. 6, A and B are points of contraflexure at sections $x = 0$ and $x = \ell$ where the bending moment is zero, while $x = x_y$ and $x = x_{ul}$ respectively indicate sections where the steel of the beam yields and the beam fails. Subscripts $y$ and $u$ refer to the yield and ultimate moment sections respectively, $x$ refers to a section at a distance $x$ from the point A and $M$ refers to the moment. Typical possible strain and force distributions at a cross section through the strengthened beam are presented in Fig. 7. When the interface lies in the tension zone of the composite element, the strain distribution profile is as shown in Fig. 7a. When the interface lies in the compression zone, the strain distribution is as shown in Fig. 7b. Fig. 7c shows the last type of strain distribution, which usually occurs when there are high values of slip at the interface resulting in tensile and compressive zones on either side of the interface.

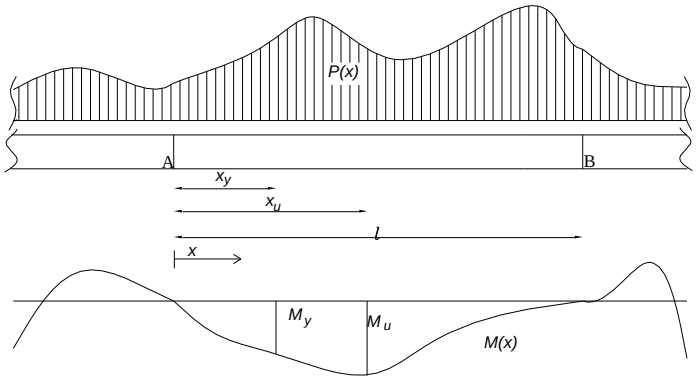


**Fig. 6** - Geometry of the beam and bending moment distribution

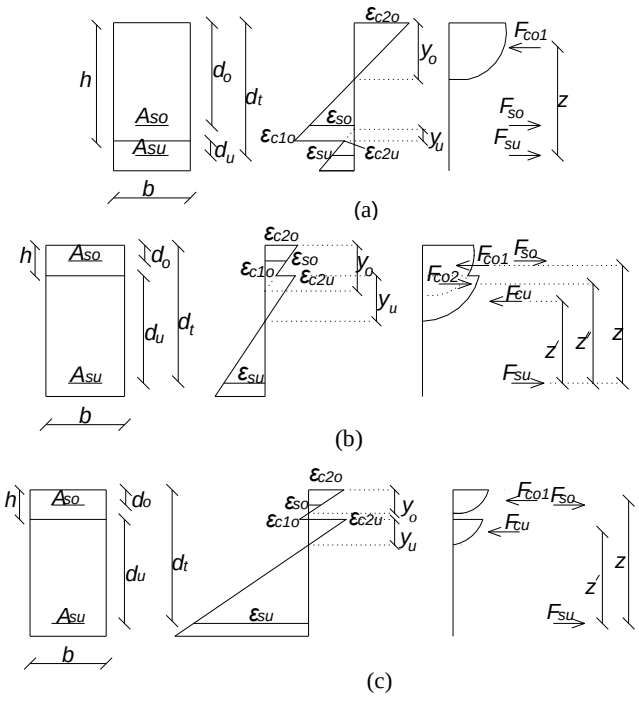

**Fig. 7** - Typical strain and force distributions of a beam with an additional new concrete layer (a) on the tensile side and (b) and (c) on the compressive side

In Fig. 7, $h$ is the distance from the top of the strengthened beam to the interface, $b$ is the width of the interface, $d_o$ is the distance of the upper component steel from the top of the beam, $d_u$ is the distance from the interface to the lower steel, $d_t$ is the distance from the top of the beam to the lower steel, $A_{so}$ and $A_{su}$ are respectively the amounts of steel in the upper and lower components of the beam, $\varepsilon_{c1o}$ and $\varepsilon_{c2o}$ are respectively the bottom and top fibre concrete strains of the upper component of the beam, $\varepsilon_{c2u}$ is the top fibre concrete strain of the lower component of the beam, $\varepsilon_{so}$ and $\varepsilon_{su}$ are respectively the steel strains of the upper and lower components of the beam, $y_o$ and $y_u$ are the neutral axis depths of the upper and lower components of the beam respectively, $z$, $z''$, $z'$ are the lever arms between the respective internal concrete forces $F_{co1}$, $F_{co2}$ and $F_{cu}$ and the force in the steel of the lower component of the beam, $F_{su}$, and $F_{so}$ is the force in the steel of the upper component of the beam.
In all following equations, strains are taken into account with their sign, positive for tensile strain and negative for compressive strain.
As stated above, it is assumed that the curvature of the upper component of the beam ($\varphi_x$) is the same as the curvature of the lower component of the beam ($\varphi_{x,u}$), that is:

$$\varphi_x = \varphi_{x,u} \tag{2}$$

Using Eq. (2), for all possible strain distribution profiles of Fig. 7, the curvature of a typical section of the strengthened element can be expressed as follows:

$$\varphi_x = \frac{\varepsilon_{c1o} - \varepsilon_{c2o}}{h} = \frac{\varepsilon_{so} - \varepsilon_{c2o}}{d_o} = \frac{\varepsilon_{su} - \varepsilon_{c2u}}{d_u} \tag{3}$$

From Fig. 7, when the interface lies in the tension zone of the composite element ($y_o < h$), or there are compressive and tensile zones on either side of the interface, the force of the upper component concrete, $F_{co}$, is equal to $F_{co1}$. When the interface lies in the compression zone, two compressive blocks define $F_{co}$ where the respective concrete forces are $F_{co1}$ and $F_{co2}$. The total concrete force of the upper component is given by Eq. (4):

$$F_{co} = F_{co1} - F_{co2} \tag{4}$$

Fig. 8 presents the force distribution in a strengthened beam subjected to bending.

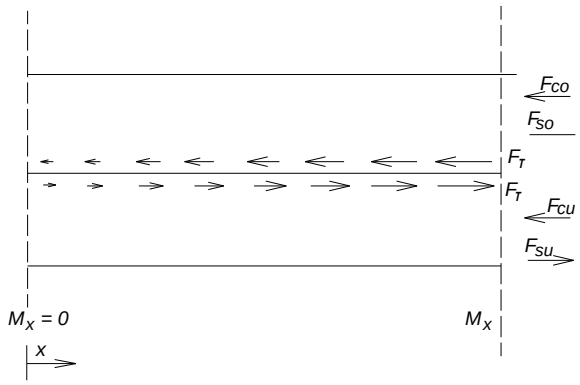


**Fig. 8** - Force distribution in a strengthened beam subjected to bending

Taking into account the equilibrium between the internal forces at any section:

$$F_{co} - F_{so} + F_{cu} - F_{su} = 0 \tag{5}$$

and the equilibrium between forces acting on the lower component of the strengthened beam can be expressed as:

$$F_{cu} - F_{su} = -F_{\tau} \tag{6}$$

Let

$$F_{co1} = 0.85 \cdot f_c \cdot b \cdot \alpha_o \cdot y_o = -0.85 \cdot f_c \cdot b \cdot \frac{\alpha_o \cdot \varepsilon_{c2o}}{\varphi_x}, \tag{7}$$

$$F_{co2} = 0.85 \cdot f_c \cdot b \cdot \alpha_1 \cdot (y_o - h) = -0.85 \cdot f_c \cdot b \cdot \frac{\alpha_1 \cdot \varepsilon_{c1o}}{\varphi_x} \tag{8}$$

and

$$\mathrm{F_{cu} = 0.85 \cdot f_c \cdot b \cdot \alpha_u \cdot y_u = -0.85 \cdot f_c \cdot b \cdot \frac{\alpha_u \cdot \varepsilon_{c2u}}{\varphi_x}} \tag{9}$$

For the cases that Figs.7a and 7c represent, $F_{co2}$ equals zero and the total compressive concrete force of the upper component is equal to $F_{co1}$.
By considering the strain distribution profiles given in Fig. 7 above and Eqs. (4), (7) and (8), $F_{co}$ is given by the following equation:

$$F_{co} = -0.85 \cdot f_c \cdot b \cdot \frac{\alpha_o \cdot \varepsilon_{c2o} - \alpha_1 \cdot \varepsilon_{c1o}}{\varphi_x} \tag{10}$$

In Eqs. (7-10), $\alpha_o$, $\alpha_1$ and $\alpha_u$ (CEN 2004) are coefficients that specify the average value of the compressive stress of each part as a fraction of the maximum acceptable compressive stress, which is equal to $0.85f_c$. Adopting the EC2 concrete stress against strain relationship (CEN 2004), values of the above coefficients can be obtained as follows:

$$\alpha_i = \begin{cases} -500 \cdot \varepsilon_{ci} \cdot (\frac{1000 \cdot \varepsilon_{ci}}{6} + 1), & for \quad 0 > \varepsilon_{ci} \geq -0.002 \\ 1 + \frac{1}{1500 \cdot \varepsilon_{ci}}, & for \quad -0.002 \geq \varepsilon_{ci} \geq -0.0035 \end{cases} \tag{11}$$

where *i* is *o*, *1* or u and $\alpha_o$ is $\alpha(\varepsilon_{c2o})$, $\alpha_1$ is $\alpha(\varepsilon_{c1o})$, $\alpha_u$ is $\alpha(\varepsilon_{c2u})$ and *ci* is *2o*, *1o* or *2u*. The steel forces are given by the following equations:

$$F_{so} = A_{so} \cdot \sigma_{so} \tag{12}$$

and

$$F_{su} = A_{su} \cdot \sigma_{su} \tag{13}$$

where $\sigma_{so}$ and $\sigma_{su}$ are the steel stresses of the upper and lower components respectively and are a function of the steel strains $\varepsilon_{so}$ and $\varepsilon_{su}$ as follows:

$$\sigma_{sj} = \begin{cases} f_{yj}, & for \quad \varepsilon_{sj} \geq f_{yj} / E_{sj} \\ \varepsilon_{sj} \cdot E_{sj}, & for \quad f_{yj} / E_{sj} \geq \varepsilon_{sj} \geq -f_{yj} / E_{sj} \\ -f_{yj}, & for \quad -f_{yj} / E_{sj} \geq \varepsilon_{sj} \end{cases} \tag{14}$$

where $j$ is $o$ for the upper component and $u$ for the under component and $\varepsilon_s$ is the steel strain.
By assuming that the shear stress at any section is a cubic function of distance $x$ (justification for this assumption can be found in Appendix A):

$$\tau_x = A1 \cdot x^3 + B1 \tag{15}$$

where $A1$ and $B1$ are constants. Then, the shear force along the interface of the strengthened beam from section A ($x = 0$, $M_x = 0$) to a section at a distance $x$ from A, is given by Eq. (16):

$$F_\tau = b \cdot \int_0^x \tau_x \, dx = \left( A1 \cdot \frac{x^4}{4} + B1 \cdot x \right) \cdot b \tag{16}$$

From Eq. (15), the average value of shear stress between the zero moment section and section $x$ ($\overline{\tau_x}$) is given by Eq. (17):

$$\bar{\tau}_x \cdot x = \int_0^x \tau_x \, dx \Rightarrow \bar{\tau}_x = A1 \cdot \frac{x^3}{4} + B1 \tag{17}$$

By considering a linear relationship between the average value of shear stress ($\bar{\tau}_m$) and the slip strain ($\varepsilon_{L,m}$) at section $x = x_{ul}$, the ultimate moment section (Dritsos 1994; Dritsos and Pilakoutas 1995; Kotsira et al. 1993; Saidi et al. 1990), it follows that:

$$\bar{\tau}_m = K \cdot \varepsilon_{L,m} \tag{18}$$

where $K$ is a coefficient expressing the relationship between $\bar{\tau}_m$ and $\varepsilon_{L,m}$.
Using the initial condition that at the ultimate moment section ($x = x_{ul}$) shear stress and as a result from Eq. (1a) slip, is equal to zero and that $\bar{\tau}_m$ at the same section is given by Eq. (17), coefficients $A1$ and $B1$ can be determined and Eq. (15) becomes:

$$\tau_x = \frac{-4}{3 \cdot x_{u,l}^3} \cdot \overline{\tau_m} \cdot x^3 + \frac{4}{3} \cdot \overline{\tau_m} \tag{19}$$

Moreover, the slip strain at any section $x$ ($\varepsilon_{L,x}$) can be defined as the concrete strain difference between the two concrete components at the interface, that is:

$$\varepsilon_{L,x} = \varepsilon_{c1o,x} - \varepsilon_{c2u,x} \tag{20}$$

Therefore, using Eqs. (1), (3-13), (16) and (18-20), the strain distribution profile at any position $x$ from a zero moment section (A or B) can be calculated.
In order to calculate the bending moment ($M_x$) at a distance $x$ from the zero moment section A, lever arms $z$, $z'$ and $z''$ need to be determined. From Fig 7 above:

$$z = d_t - C_o \cdot y_o = d_t - C_o \cdot (\frac{-\varepsilon_{c2o}}{\varphi_x}) = d_t + C_o \cdot \frac{\varepsilon_{c2o}}{\varphi_x}, \quad (21)$$

$$z' = d_u - C_u \cdot y_u = d_u + C_u \cdot \frac{\varepsilon_{c2u}}{\varphi_x} \quad (22)$$

and

$$z'' = d_u - C_1 \cdot (y_o - h) = d_u + C_1 \cdot \frac{\varepsilon_{c1o}}{\varphi_x} \quad (23)$$

where $C_o$, $C_1$ and $C_u$ are coefficients that specify the centre weight distance of $F_{co1}$, $F_{co2}$ and $F_{cu}$ from the top of each component as a function of $\varepsilon_{c2o}$, $\varepsilon_{c1o}$ and $\varepsilon_{c2u}$ respectively and are given by Eq. (24) (CEN 2004).

$$C_i = \begin{cases} \dfrac{(1+125\cdot\varepsilon_{ci})}{(3+500\cdot\varepsilon_{ci})}, & for \quad 0 > \varepsilon_{ci} \geq -0.002 \\ \dfrac{1000\cdot\varepsilon_{ci}\cdot(3000\cdot\varepsilon_{ci}+4)+2}{2000\cdot\varepsilon_{ci}\cdot(3000\cdot\varepsilon_{ci}+2)}, & for \quad -0.002 \geq \varepsilon_{ci} \geq -0.0035 \end{cases} \quad (24)$$

where *i* and *ci* are as previous defined for Eq. (11).
Therefore, the bending moment at a distance *x* is as follows:

$$M_x = F_{co1}\cdot z - F_{co2}\cdot z'' + F_{cu}\cdot z' - F_{so}\cdot(d_t - d_o) \Rightarrow$$

$$\begin{aligned} M_x = & -0.85\cdot f_c \cdot b \cdot \alpha_o \cdot \frac{\varepsilon_{c2o}}{\varphi_x}\cdot(d_t + C_o \cdot \frac{\varepsilon_{c2o}}{\varphi_x}) \\ & + 0.85\cdot f_c \cdot b \cdot \alpha_1 \cdot \frac{\varepsilon_{c1o}}{\varphi_x}\cdot\left(d_u + C_1 \cdot \frac{\varepsilon_{c1o}}{\varphi_x}\right) \\ & - 0.85\cdot f_c \cdot b \cdot \alpha_u \cdot \frac{\varepsilon_{c2u}}{\varphi_x}\cdot(d_u + C_u \cdot \frac{\varepsilon_{c2u}}{\varphi_x}) - A_{so}\cdot\sigma_{so}\cdot d_t(1-\frac{d_o}{d_t}) \end{aligned} \quad (25)$$

By assuming that at the ultimate section the top fibre concrete strain is equal to -0.0035 and by assuming a value of curvature of $\varphi_x$ equal to the value of curvature of a monolithic element, Eqs. (3), (5) and (6) can be used to calculate the concrete and steel strains. Next, coefficients $\alpha_o$, $6\alpha_1$, $\alpha_u$, $C_o$, $C_1$ and $C_u$ and steel stresses $\sigma_{so}$ and $\sigma_{su}$ can be determined using Eqs. (11), (24) and (14) respectively. Then, by using trial and error, iteration and Eqs. (9)-(13), the concrete and steel forces can be calculated. If Eq. (5) is satisfied, results are acceptable and the ultimate bending moment can be determined using Eqs. (21)-(24). If results do not satisfy Eq. (5), a new value for the curvature is assumed and the procedure is repeated until force equilibrium at the section and at the interface is achieved.
The same procedure can be repeated for the steel strain at the yield section ($\varepsilon_{so}$ or $\varepsilon_{su} = f_y/E_s$, whichever yields first) rather than using $\varepsilon_{c2o}$ = -0.0035. Therefore, the section of steel yield ($x_y$), the yield moment ($M_y$) and the yield curvature ($\varphi_y$) can also be determined.
The slip strain at a section *x* ($\varepsilon_{L,x}$) can be found from the following equation (see Fig. 7 and Eq. (20) above):

$$\varepsilon_{L,x} = \varepsilon_{c1o,x} - \varepsilon_{c2u,x} = \Delta_x \cdot \varphi_x \quad (26)$$

where $\Delta_x$ is a function which gives the relationship between the slip strain and the curvature at any section at a distance of $x$ from section A.
Assuming that at section $x_{ul}$, where the bending moment takes its maximum value, $\Delta_x$ also takes a maximum value of $\Delta_m$ and the value of the curvature is equal to $\varphi_u$. Therefore, at section $x_{ul}$ for strengthening on the tensile side (Fig. 7a above):

$$\varepsilon_{L,m} = \varepsilon_{c1o,m} - \varepsilon_{c2u,m} = (h - y_{o,m} - y_{u,m}) \cdot \varphi_u = \Delta_m \cdot \varphi_u \tag{27a}$$

and for strengthening on the compressive side (Figs. 7b and 7c)

$$\varepsilon_{L,m} = \varepsilon_{c1o,m} - \varepsilon_{c2u,m} = (h - y_{o,m} + y_{u,m}) \cdot \varphi_u = \Delta_m \cdot \varphi_u \tag{27b}$$

By assuming a linear distribution of $\Delta$ along the length of the beam, at any section $x$ of the strengthened beam, respective values for coefficient $\Delta_x$ can be calculated as follows:

$$\Delta_x = \frac{\Delta_m}{x_{ul}} \cdot x \tag{28}$$

where

$$\Delta_m = (h - y_{o,m} - y_{u,m}) = \Delta_{x=x_{ul}} \tag{29a}$$

for strengthening on the tensile side,

$$\Delta_m = (h - y_{o,m} + y_{u,m}) = \Delta_{x=x_{ul}} \tag{29b}$$

for strengthening on the compressive side and $\varepsilon_{L,x=0} = 0 \Rightarrow \Delta_{x=0} = 0$.
A typical bending moment against curvature plot can be idealized for simplicity as bilinear, as shown in Fig. 9. From Fig. 9, two different cases can be distinguished: a) the case when the examined section is before the yield section ($M_x \leq M_y$ for $x \leq x_y$) and b) the case when the examined section is after the yield section ($M_x \geq M_y$ for $x \geq x_y$).

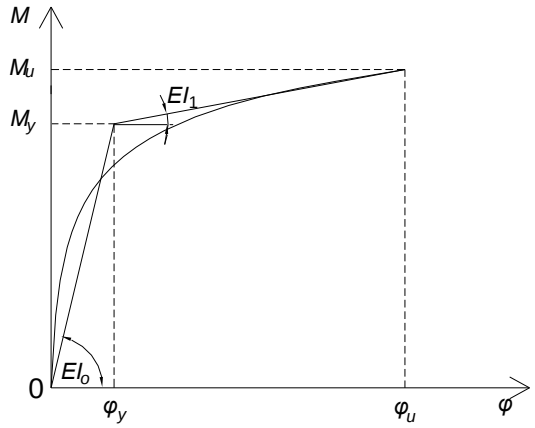


**Fig. 9** - Bilinear idealization of the bending moment against curvature plot

In Fig. 9, $EI_o$ is the elastic stiffness of the strengthened beam, $EI_1$ is the inelastic stiffness of the strengthened beam, $M_y$ is the bending moment when the steel of the beam begins to yield ($x = x_y$), $M_u$ is the ultimate bending moment at $x = x_{ul}$ and $\varphi_y$ and $\varphi_u$ are the respective yield and ultimate curvatures.
By considering a section at a distance of $x$ less than $x_y$, the curvature is as follows:

$$\varphi_x = \frac{M_x}{EI_o} \tag{30}$$

It is assumed that the beam is reinforced so that the steel would yield before the ultimate strength of the element is reached ($x_y < x_{ul}$).
From Eqs. (26), (28) and (30) the slip strain is given by:

$$\varepsilon_{L,x} = \Delta_x \cdot \varphi_x \Rightarrow \varepsilon_{L,x} = \frac{2 \cdot \Delta_m \cdot M_x}{EI_o \cdot \ell} \cdot x \text{, for } 0 \le x \le x_y \tag{31}$$

Therefore, the slip can be obtained from:

$$s_x = \int_0^x \varepsilon_{L,x} dx = \int_0^x \left( \frac{2 \cdot \Delta_m \cdot M_x}{EI_o \cdot \ell} \cdot x \right) dx, \text{ for } 0 \le x \le x_y \tag{32}$$

and by considering Eqs. (1a) and (32):

$$\tau_x = k_s \cdot \int_0^x \left( \frac{2 \cdot \Delta_m \cdot M_x}{EI_o \cdot \ell} \cdot x \right) dx, \text{for } 0 \le x \le x_y \tag{33}$$

From the bilinear idealization of Fig. 9, when $x_y \le x \le x_{ul}$, the inelastic stiffness is given by:

$$EI_1 = \frac{M_x - M_y}{\varphi_x - \varphi_y} \tag{34}$$

By rearranging Eq. (34), the following equation for the curvature at any section $x$ between $x_y \le x \le x_{ul}$ can be obtained:

$$\varphi_x = \frac{M_x - M_y}{EI_1} + \varphi_y \tag{35}$$

By considering Eqs. (26), (28) and (35), the slip strain is given as follows:

$$\varepsilon_{L,x} = \left( \frac{M_x - M_y}{EI_1} + \varphi_y \right) \cdot \frac{2 \cdot \Delta_m}{\ell} \cdot x, \text{ for } x_y \le x \le x_{ul} \tag{36}$$

Moreover, from Eqs. (32) and (35):

$$s_x = \int_x \varepsilon_{L,x} dx \Rightarrow$$

$$s_x = \int_0^{x_y} \left( \frac{2 \cdot \Delta_m \cdot M_x}{EI_o \cdot \ell} \cdot x \right) dx + \int_{x_y}^x \left[ \left( \frac{M_x - M_y}{EI_1} + \varphi_y \right) \cdot \frac{2 \cdot \Delta_m}{\ell} \cdot x \right] dx, \tag{37}$$

$$\text{for} \quad x_y \le x \le x_{ul}$$

In addition, from Eqs. (1) and (37):

$$\tau_x = k_s \cdot \left\{ \int_0^{x_y} \left( \frac{2 \cdot \Delta_m \cdot M_x}{EI_o \cdot \ell} \cdot x \right) dx + \int_{x_y}^x \left[ \left( \frac{M_x - M_y}{EI_1} + \varphi_y \right) \cdot \frac{2 \cdot \Delta_m}{\ell} \cdot x \right] dx \right\}, \tag{38}$$

$$\text{for } x_y \le x \le x_{ul}$$

If for the ultimate strength of the element there is not steel yield, the relationship between bending moment $M_x$ and curvature $\varphi_x$ is linear according to Eq. (30) and the slip strain, slip and shear stress distribution along the interface of the strengthened element, are given by Eqs. (31-33).
It should also be mentioned that, the whole procedure can be used for every other phase, except of ultimate limit state, in which maximum value of bending moment is known. The only difference is that at section at $x_{ul}$ distance from A the bending moment $M_{max}$ instead of concrete strain $\varepsilon_{c2o}$ is now given.
By assuming that the relationship between the shear stress and slip is given by Eq. (1a), the shear stress at the zero moment section A ( $\tau_A$ ) is given by $\tau_A = k_s \cdot s_A$ where $s_A$ is the slip at section A. Furthermore, the maximum slip occurs at sections A and B, the sections of zero moment, and can be approximated by the following equation:

$$s_A = s_B = \overline{\varepsilon_L} \cdot x_{ul} = a_1 \cdot \varepsilon_{L,m} \cdot x_{ul} \tag{39}$$

where $\overline{\varepsilon_L}$ is the average value of slip strain from the zero moment section to the ultimate moment section, $a_1$ is a coefficient that depends on the distribution of slip strain along the strengthened beam and $\varepsilon_{Lm}$ is the slip strain at the ultimate moment section of the beam.
The slip strain at the ultimate moment section of the composite beam can be evaluated by using Eqs. (3), (5), (6), (12), (13), (16) and (20) for $x = x_{ul}$.
Additionally:

$$\bar{\tau}_m = a_2 \cdot \tau_A \tag{40}$$

where $a_2$ is a coefficient that depends on the distribution of shear stress along the strengthened beam. Using Eqs. (18), (39) and (40), the shear stress at sections A and B is given by the following equation (denoting $a_1 \cdot a_2$ as $a_{1,2}$):

$$\tau_A = \tau_B = \frac{1}{a_1 \cdot a_2} \cdot K \cdot \frac{s_A}{x_{ul}} = \frac{1}{a_{1,2}} \cdot K \cdot \frac{s_A}{x_{ul}} \tag{41}$$

By comparing Eqs. (1a) and (41), it can be seen that:

$$K = a_{1,2} \cdot x_{ul} \cdot k_s \tag{42}$$

Obviously, by definition $a_{1,2} < 1.0$. However, it should be noted that in the most practical cases examined in the framework of this research, values of coefficient $a_{1,2}$ were found to range from 0.2 to 0.3.

# 6. Analytical Procedure

According to the above analysis, an iterative procedure is required to define the distribution of slip along the interface of a strengthened beam. The procedure encompasses the following steps:
**Step 1:** Input and assumption data.
A $\tau$ against $s$ interface model, as in Fig. 5 above or as experimentally determined, is adopted regarding the type of the interface (smooth, rough, reinforced or unreinforced). The choice could be made to start with any possible $k_s$ between 1.0 MPa/mm and 2.0 MPa/mm. Alternatively, in cases where low values of interface shear stresses are expected (lower than $\tau_1$), it is better to start with $k_s = k_{s,o}$. In addition, a value for $a_{1,2} \leq 1.0$ is assumed. A reasonable value to begin with

would be $a_{1,2}$ in the range of 0.2 to 0.3. Coefficient $K$ is then calculated from Eq. (42).

**Step 2:** Ultimate moment section internal forces and strain distribution.
Using Eqs. (4)-(13), (16) and (18) and assuming that failure occurs when $\varepsilon_{c2o}$ equals -0.0035, the strain distribution profile at the section $x_{ul}$ of ultimate moment and the resulting strains ($\varepsilon_{c1o}$ and $\varepsilon_{c2u}$), the ultimate moment ($M_u$) and the ultimate curvature ($\varphi_u$) can be calculated. Substituting results from the strain distribution profile into Eqs. (29a) or (29b), coefficient $\Delta_m$ can be determined.

**Step 3:** Yield section internal forces and strain distribution.
Using Eqs. (4)-(20), coefficient $K$ from step 1, $M_u$ from step 2 and by assuming the yield section is the section where the steel strain equals the steel yield strain ($\varepsilon_{sy}$), the distance between the zero moment section and the yield section ($x_y$), the moment at yield ($M_y$) and the curvature at yield ($\varphi_y$) can be calculated. Here, two cases can be examined. Either the steel of the initial beam or the steel of the additional layer yields first and one of these two cases can be eliminated. By first assuming the steel strain of the initial beam is at the yield point, it can be determined if the steel strain of the additional layer is below or above the yield point. If the steel strain of the additional layer is found to be above the yield point, it means that this steel would yield first.

**Step 4:** Initial shear stress and slip strain distribution.
Using the results from steps 2 and 3 with Eqs. (30) and (33), $EI_o$ and $EI_1$ can be calculated. Now, the slip strain and shear stress distributions along the interface of the strengthened beam can be determined using Eqs. (31)-(33) and (36)-(38). According to these distributions, $\varepsilon_{L,m}$ and $\tau_A$ are the maximum values of slip strain and shear stress respectfully and, using Eq. (32), the maximum slip value $s_A$ can be determined.

**Step 5:** Verification of $a_{1,2}$ value.
Coefficients $a_1$ and $a_2$ can be calculated from the distributions of step 4. If $a_{1,2}$ is found to be close to the value assumed in step 1, the results of step 4 are correct. If not, the whole procedure is repeated from step 1 using the new $a_{1,2}$ value. Iterations stop when the result of step 4 is almost the same as the assumption of step 1.

**Step 6:** Verification of the stiffness $k_s$ value.
By considering that $\tau_x = \tau_A$ and using the $\tau$ against $s$ curve adopted in step 1, a corresponding slip value ($s_x$) can be calculated. If $|s_A - s_x| / s_A \le 5\%$, the initially assumed value of $k_s$ is acceptable. Using Eq. (1), $\tau_A$ and $s_x$, a new value for coefficient $k_s = \tau_A/s_x$ can be determined and the whole procedure from steps 2 to 5 is iteratively repeated until the values of $s_A$ and $s_x$ are found to be very close.

**Step 7:** Slip distribution.
From Eq. (19), a $\tau_A$ value can be obtained by substituting $\overline{\tau_m} = K \cdot \varepsilon_{L,m}$. If this shear stress value is close to that as obtained in step 6, the shear stress, the slip strain and the slip distribution of step 6 is valid. If not, the whole procedure is repeated with a new Eq. (19) obtained from Eqs. (15) and (17) considering that for $x = x_{ul}$, $\tau_x = 0$ and $\overline{\tau_m}$ is the value obtained from shear stress distribution of step 4.

# 7. Verification of the method

For verification purposes, the method is compared to both experimental results and finite element analysis. The beam investigated by Loov and Patnaik (1994)

was chosen for this purpose and was analyzed using the method proposed in this paper and the finite element method.
The beam of Loov and Patnaik (1994) was a simply supported T concrete beam consisting of two concrete elements, loaded with a concentrated load at the mid span of the beam. The web portion was first fabricated with a rectangular cross section of 150 mm by 230 mm with 1600 mm$^2$ tensile reinforcement and 55 mm cover (Fig. 10). The flange was cast in place over the web and had a cross section of 400 mm by 120 mm. The yield strength of the reinforcement was found to be 454 MPa, while the concrete strength was 38.0 MPa for the initial beam and 35.6 MPa for the flange.
For the connection between the two elements, the $\tau$ against $s$ relationship was found experimentally by Loov and Patnaik (1994) and is presented in Fig. 11. This experimental $\tau$ against $s$ interface relationship was adopted for the analysis.

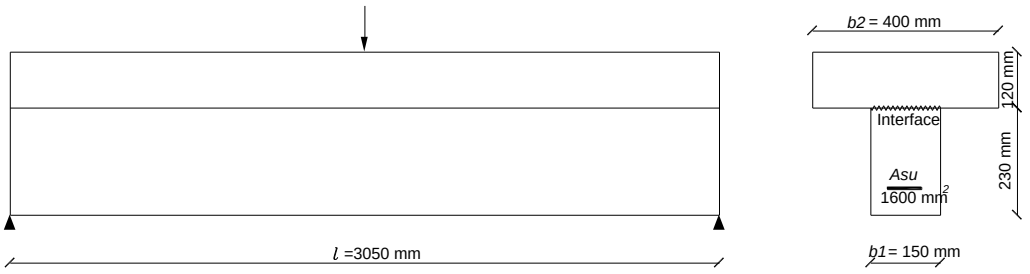


**Fig. 10** - Geometry and loading condition for the beam strengthened with concrete layer on the compressive side (Loov and Patnaik 1994)

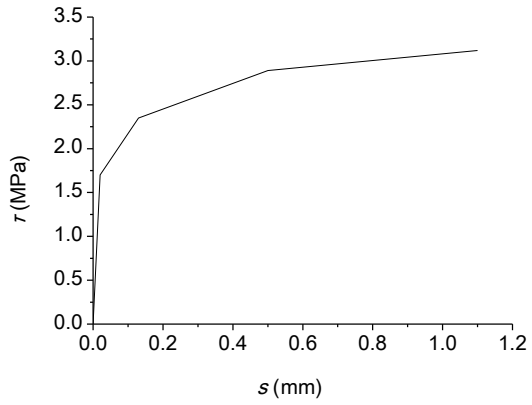


**Fig. 11** - Experimental $\tau$ against interface $s$ curve (Loov and Patnaik 1994)

As the beam in question was a T beam, $F_t$, and $F_{cu}$ are determined by considering that $b = b_1 = 150$ mm, while $F_{co}$, $F_{co1}$ and $F_{co2}$ are determined by considering $b = b_2 = 400$ mm. In order to illustrate the application of the described analytical method, the seven-step procedure proposed above is followed.
**Step 1:** Input and assumption data.
Initially, assume that $a_{1,2} = 0.3$ and $k_s = 1.1$ MPa/mm. Therefore, from Eq. (42), $K = 0.3 \cdot 1.1 \cdot 1525 = 503$ MPa.
**Step 2:** Ultimate moment section internal forces and strain distribution.
From Eqs. (4)-(13), (16) and (18) and assuming that at the ultimate stage $\varepsilon_{c2o} = -0.0035$, the strain distribution profile at the ultimate moment section ($x_u = \ell / 2 = 1525$ mm) is obtained as shown in Fig. 12a, where $y_{o,m} = 62.7$ mm, $y_{u,m} = 45.0$ mm and $\varepsilon_{L,m} = \varepsilon_{c1o} - \varepsilon_{c2u} = 0.00319-(-0.00251) = 0.00570$.

Consequently, from Eq. (29b), $\Delta_m$ = 102 mm, from Eq. (25), $M_u$ = 200 kNm and from Eq. (3), $\varphi_u$ = 0.0558 m$^{-1}$. It can also be determined from Eq. (18) that $\overline{\tau_m}$ = $503 \cdot 0.0057 = 2.87$ MPa.

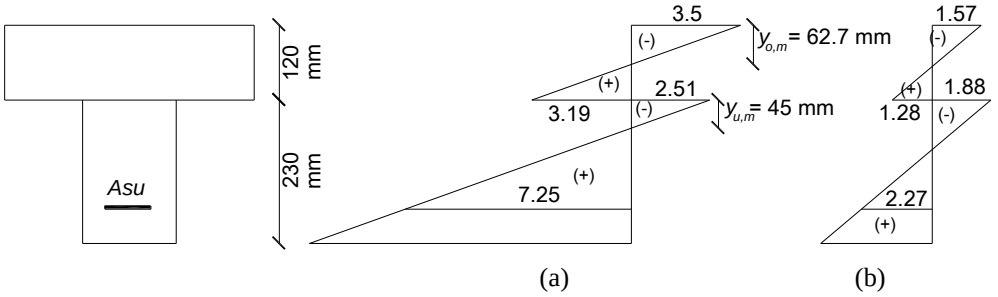


**Fig. 12** - Strain (x10$^{-3}$) distribution profile a) at the ultimate moment section and b) at the yield section

**Step 3:** Yield section internal forces and strain distribution.
Using Eqs. (4)-(20), setting $K$ = 503 MPa from step 1, $M_u$ = 200 kNm and $\varepsilon_{L,m}$ = 0.00570 from step 2 and assuming that the yield point is when $\varepsilon_{su} = f_y/E_s$ = 0.00227, the distance between the zero moment section and the yield section ($x_y$), the moment at yield ($M_y$) and the curvature at yield ($\varphi_y$), using Eqs (6), (9), (13) and (16), (25) and (3), are determined to be $x_y$ = 913 mm, $M_y$ = 168 kNm and $\varphi_y$ = 0.0240 m$^1$. Fig 12b above presents the yield section strain distribution.
**Step 4:** Initial shear stress and slip strain distribution.
Using steps 2 and 3 results and from Eqs. (30) and (34), $EI_o$ and $EI_1$ are calculated to be 7.00x10$^3$ kNm$^2$ and 1.01x10$^3$ kNm$^2$ respectively and using Eqs. (31) and (36) and Eqs. (33) and (38), the slip strain and the shear stress distribution can be found as in Figs. 13a and 13b. From these figures, maximum values are $\tau_A$ = 3.09 MPa and $\varepsilon_{L,m}$ = 5.70x10$^{-3}$. From Eq. (32), it can be determined that $s_A$ = 2.81 mm.

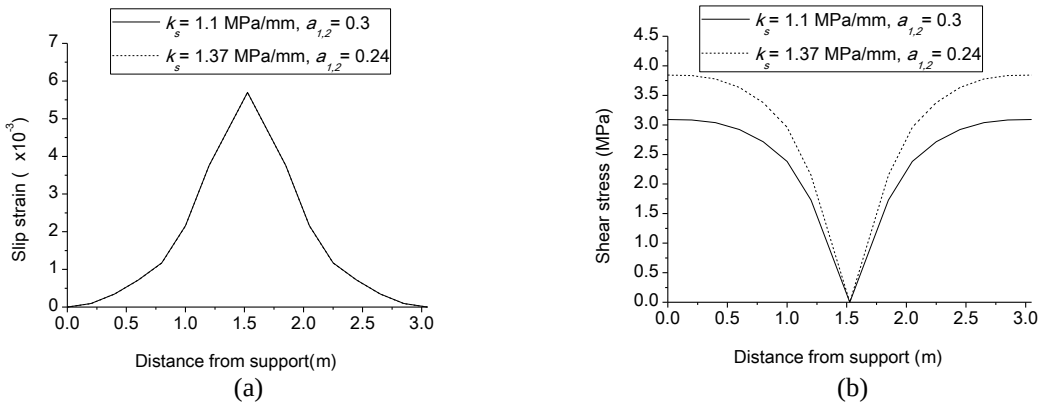


**Fig. 13** - Distributions a) of slip strain and b) of shear stress, along the interface of the strengthened beam for $k_s$ = 1.1 MPa/mm and $a_{1,2}$ = 0.3 and $k_s$ = 1.37 MPa/mm and $a_{1,2}$ = 0.240

**Step 5:** Verification of the $a_{1,2}$ value.
From the slip strain and shear stress distributions of Fig. 13, the average values of slip strain and shear stress can be calculated as $\overline{\varepsilon_L} = \frac{\int_0^{1.525} \varepsilon_L(x)}{1.525} = 1.84 \cdot 10^{-3}$ and

$\bar{\tau} = \frac{\int_0^{1.525} \tau(x)}{1.525} = 2.35\,\text{MPa}$. Therefore, $a_1 = \frac{\bar{\varepsilon}_L}{\varepsilon_{L,m}} = \frac{1.84}{5.70} \Rightarrow a_1 = 0.323$ and

$a_2 = \frac{\bar{\tau}}{\tau_A} = \frac{2.35}{3.09} = 0.761$. Consequently, $a_{1,2} = 0.323 \cdot 0.761 = 0.246 \neq 0.300$.

The whole procedure is repeated using $a_{1,2} = 0.246$. It is finally determined that $a_{1,2} = 0.240$ is correct and $K = 0.240 \cdot 1.1 \cdot 1525 = 403\,\text{MPa}$ the maximum slip $s_A$ = 3.3 mm and the maximum shear stress $\tau_A$ = 3.63 MPa.

**Step 6:** Verification of the stiffness $k_s$.

For $\tau_A$ = 3.63 MPa and from the theoretical curve adopted in step 1 (Fig.11 above), $s_{A,n}$ = 2.40 mm and $|s_A - s_{A,n}| / s_A = 27\% > 5\%$. Therefore, the whole procedure (steps 2 to 5) is repeated using $k_s = \tau_A / s_{A,n}$ = 3.63/2.40 = 1.51 MPa/mm.

The process is repeated until there is a converge between $s_{A,n}$ and $s_A$.

After some iterations, it is found that $k_s$ = 1.37 MPa/mm, $K$ = 501 MPa, $s_A$ = 2.80 mm, $\tau_A$ = 3.84 MPa and $\varepsilon_{L,m}$ = 0.00570. From the $\tau$ against $s$ curve adopted in step 1, for $\tau_A$ = 3.84 MPa, it is found that $s_{A,n}$ = 2.90 mm and $|s_A - s_{A,n}| / s_A = 3.6\% < 5\%$, an acceptable difference. The slip strain, shear stress and slip distribution for this case are presented in Figs. 13 and 14. From the shear stress distribution of Fig. 13b, $\overline{\tau_m} = 2.90$ MPa.

**Step 7:** Final slip distribution.

From Eq. (19), by substituting $\overline{\tau_m} = K \cdot \varepsilon_{L,m} = 501 \cdot 0.0057 = 2.86\,\text{MPa}$ a value of $\tau_A$ = 3.81 MPa is obtained. This shear stress value is almost equal to the value of $\tau_A$ obtained in step 6. Therefore, the shear stress, the slip strain and the slip distributions of step 6 are valid and the results of this step can be considered as acceptable.

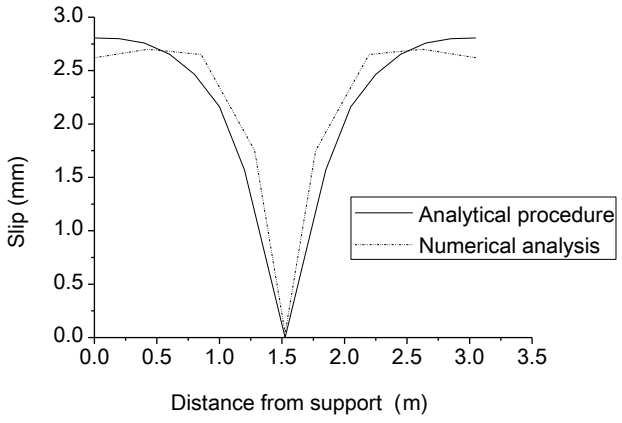


**Fig. 14** - Distribution of slip along the interface of the strengthened beam

From Figs. 13 and 14, the distribution of slip and shear stress along the interface of the beam was found to be almost parabolic with maximum values at the supports and minimum values at the mid span. Furthermore, from the distribution of slip strain along the interface, maximum values occur at mid span and minimum values occur at the supports.

## 7.1 Comparison with experimental results

For the above experimentally tested beam, Loov and Patnaik (1994) reported that the maximum slippage recorded at the support section was "*greater than 2 mm*". Therefore, the analytical maximum slip value of 2.80 mm found above through the proposed method can be considered in good agreement with the experimental result. Furthermore, Loov and Patnaik (1994) approximately evaluated the maximum shear stress experimental value as 3.12 MPa, which is close to value of 3.84 MPa obtained from the present analytical method.

## 7.2 Comparison with numerical analysis

In the following, the analytical results of the proposed method are compared with respective numerical results. Firstly, the beam of Loov and Patnaik (1994) is examined. Then, a simply supported rectangular concrete beam strengthened by adding a concrete layer to the tensile side, as described in Appendix A, is examined considering a number of possible interface conditions. For the numerical analysis, the ATENA (2005) finite element program was used. Fig. 15 presents the adopted models for the concrete and steel reinforcement.

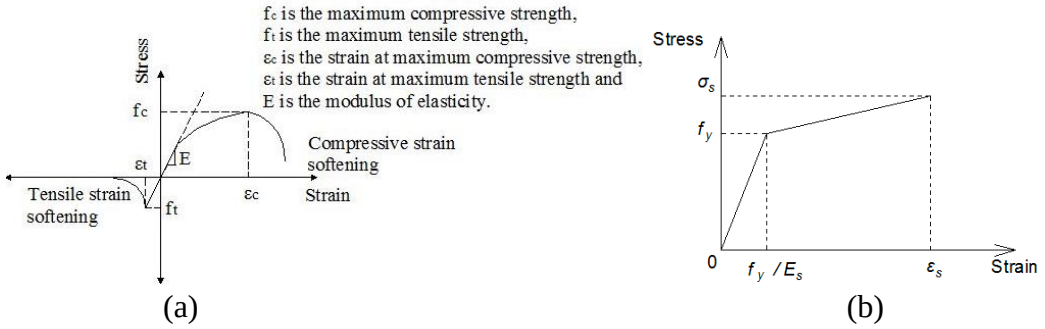


**Fig. 15** – a) Concrete and b) steel model (adopted for the numerical analysis)

Solid elements were used to simulate the concrete using the stress against strain behaviour in compression proposed by CEB-FIP Model Code (1990), as shown in Fig. 15a. The element used to simulate the reinforcement (Fig. 15b) was a link element with bilinear stress against strain behaviour, strain hardening and relative slip with the concrete element using the bond model proposed by the CEB-FIP Model Code (1990). The interface between the old and new concrete was simulated using special contact elements (a pair of two elements) considering appropriate values for the coefficients of friction $\mu$ and adhesion $c$ regarding the interface type (Lampropoulos and Dritsos 2008).

For the numerical analysis of the tested beam, values of $\mu$ = 1.0 and $c$ = 1.0 MPa were adopted as the interface in the Loov and Patnaik (1994) experiment was rough. The numerical results for the maximum interface shear stress and the maximum slippage, are 3.89 MPa and 2.60 mm respectively. Comparing analytical and numerical results for the slip distribution, as presented above in Fig. 14, very good agreement can be observed.

For the numerical analyses of the strengthened rectangular concrete beam (details are presented in Appendix A), six cases concerning six different interface conditions were examined. Namely: a) $\mu$ = 0.5, $c$ = 0.0 MPa, b) $\mu$ = 0.5, $c$ = 0.5 MPa, c) $\mu$ = 0.5, $c$ = 1.0 MPa, d) $\mu$ = 1.0, $c$ = 0.0 MPa, e) $\mu$ = 1.5, $c$ = 0.0 MPa and f) $\mu$ = 1.5, $c$ = 1.0 MPa.

For the numerical analyses, the above coefficients of friction and adhesion were used to derive different $\tau$ against $s$ relationships at the support positions, which were then used in the analytical work.
In Fig. 16, numerical results of two characteristic cases (case b: $\mu = 0.5$ $c = 0.5$ MPa and case f: $\mu = 1.5$ $c = 1.0$ MPa) are demonstrated.

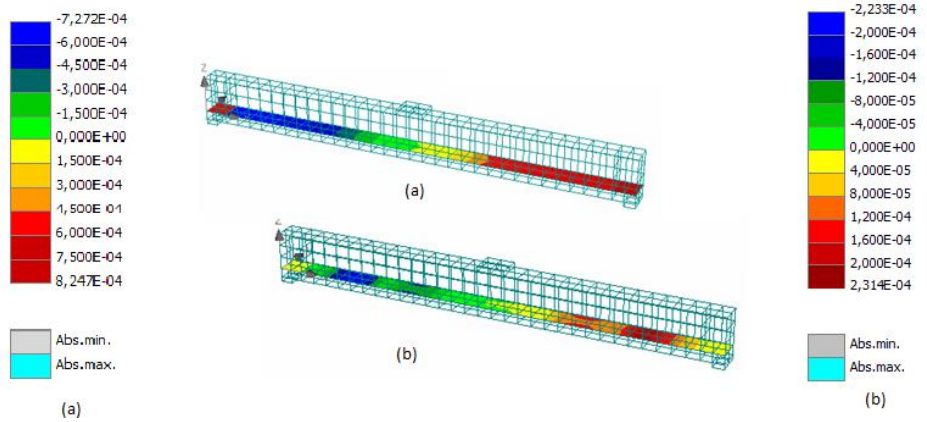


**Fig. 16 –** Numerical slip distribution at the interface a) case b and b) case f

In Fig. 17, numerical and analytical results concerning the maximum slippage of each case examined are compared and very good agreement can be seen.

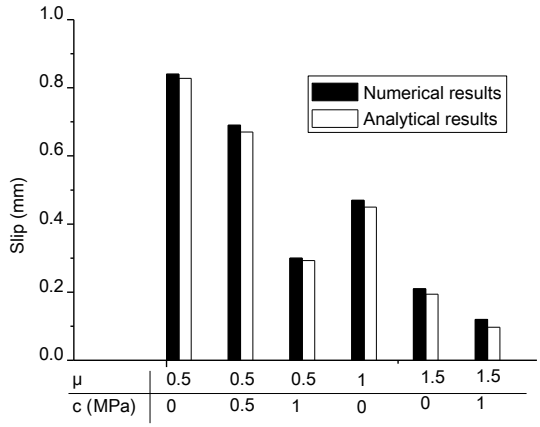


**Fig. 17 –** Comparison between analytical and numerical maximum slip at the interface

Obviously, very good agreement between analytical and numerical results has been demonstrated.

# 8. Conclusions

The practice of adding a new concrete layer to the compressive or tensile side of an element is a technique that is used to strengthen concrete elements that are weak in flexure and has been the object of many experimental investigations. However, a model has not yet been presented in the literature to evaluate the slip between the two components. In common practical design, slip is ignored and strengthened elements are assumed monolithic. Ignoring slip at the interface may not be a conservative assumption.
The present study has developed general equations to calculate the distribution of slip, shear stress and slip strain at the interface between two reinforced concrete

components. An accurate procedure for calculating the distribution of slip, shear stress and slip strain along the length of the interface has been presented. It was found that there is a relationship between the slip strain and the slip at the interface, which is given approximately through the relationship between the two coefficients $K$ and $k_s$. Here, $K$ is the average value of the shear stress divided by the slip strain at ultimate moment section and $k_s$ is the shear stress divided by the slip at any section at a distance x from a section of zero moment. When the procedure was applied to a simply supported beam example, the distribution of slip and shear stress along the interface of the beam was found to be almost parabolic with maximum values at the supports and minimum values at the mid span. Furthermore, from the distribution of slip strain along the interface, maximum values occur at mid span and minimum values occur at the supports. When comparing results of analytical procedure with respective experimental and numerical ones, a good agreement was observed.
Finally, further results of the proposed analytical procedure concerning a rectangular concrete beam strengthened with a concrete layer at its tensile side were checked using ATENA (2005) software for different types of the interface. The comparison between maximum slip at the interface of the strengthened beam showed very good agreement.

## Acknowledgments

The authors would like to thank Dr V. J. Moseley for his significant assistance during the preparation of this manuscript.

## References

[1] ACI Committee 209, Subcommittee 2 (1971) Prediction of creep, shrinkage and temperature effects in concrete structures. Designing for effects of creep, shrinkage and temperature effects in concrete structures. American Concrete Institute, Detroit
[2] ACI Committee 318 (2004) Building code requirements for structural concrete and commentary. American Concrete Institute, Farmington Hills, Michigan
[3] ATENA (2005) ATENA program documentation 2005. Cervenka Consulting Prague (Czech Republic)
[4] Altun F (2004) An experimental study of jacketed reinforced concrete beams under bending. Construction and Building Materials 18:611-618. doi:10.1016/j.conbuildmat.2004.04.0005
[5] Banta T (2005) Horizontal shear transfer between ultra high performance concrete and lightweight concrete. Master of Science in Civil Engineering, Virginia Polytechnic Institute and State University
[6] Bass RA, Carrasquillo RL, Jirsa JO (1985) Interface shear capacity of concrete surfaces used in strengthening structures. Report on a research project. Department of Civil Engineering, University of Texas
[7] Beushausen H. and Alexander M.G. (2006) Failure mechanisms and tensile relaxation of bonded concrete overlays subjected to differential shrinkage. Cement and Concrete Research, 36:1908-1914. doi:10.1016/j.cemconres.2006.05.027
[8] Beushausen H. and Alexander M.G. (2007) Localised strain and stress in bonded concrete overlays subjected to differential shrinkage. Materials and Structures, 40:189-199. doi:10.1617/s11527-006-9130-z
[9] Birkeland HW (1960) Differential shrinkage in composite beams. ACI Journal, 56:1123-1136
[10] Birkeland PW, Birkeland HW (1966) Connections in precast concrete construction. ACI Journal, 63:345-367
[11] BS 8110-1: 1992 (1995) Structural use of concrete. British Standards Institute, London.
[12] CEB Bulletin No 162 (1983) Assessment of concrete structures and design procedures for upgrading. Comite Euro-International du Beton, Paris
[13] CEB-FIP (1993) Model Code 1990 Design Code. Comite Euro-international du Beton, Thomas Telford Ltd., London

[14] CEB-FIP (2008) Structural connections for precast concrete buildings. Comite Euro-International du Beton, Bulletins d'Information No. 43. Thomas Telford, London
[15] CEN (2004) En 1992-1-1, Eurocode 2: Design of concrete structures-Part 1-1: General rules and rules for buildings. European Committee for Standardization, Brussels
[16] CEN (1998) En 1998-1-4, Eurocode 8: Design provisions for earthquake resistance of structures-Part 1-4:Strengthening and repair of buildings. European Committee for Standardization, Brussels
[17] CEN (2005) En 1998-3, Eurocode 8: Assessment and retrofitting of buildings. European Committee for Standardization, Brussels
[18] Cheong HK, MacAlevey N (2000) Experimental behaviour of jacketed reinforced concrete beams. ASCE Journal of Structural Engineering, 126:692-699
[19] CSA A23.3 (1994) Design of concrete structures for buildings. Canadian Standards Association, Rexdale, Ont., Canada
[20] Dimitriadou O, Kotsoglou V, Thermou G, Savva A, Pantazopoulou S (2005) Experimental study of concrete interfaces in sliding shear. Tech. Chron. Sci. J. TCG, No 2-3:123-136 (in Greek)
[21] Dritsos S (1994) Ultimate strength of flexurally strengthened RC members. Proceedings of the 10th European Conference on Earthquake Engineering, Vienna, 1637-1642
[22] Dritsos S, Pilakoutas K (1995) Strengthening of RC elements by new concrete layers. European Seismic Design Practice, Proceedings of the 5th SECED Conference, Chester, 611-617
[23] Dritsos S (1996) Strengthening of RC beams by new cement based layers. Proceedings of the International Conference: Concrete Repair Rehabilitation and Protection, Dundee, Scotland, 515-526
[24] Dritsos S (2007) Seismic strengthening of columns by adding new concrete. Bulletin of the New Zealand Society for Earthquake Engineering, 40(2):49-67
[25] Dritsos S, Vandoros C, Agelopoulos G, Antonogiannaki E, Tzana M (1996) Shear transfer mechanism at interface between old and new concrete. Proceedings of the 12th Greek Conference on Concrete, Nicosia, Cyprus, 200-213 (in Greek)
[26] GRECO (2009) Greek Retrofitting Code. Third draft version by the Greek Organization for Seismic Planning and Protection. Greek Ministry for Environmental Planning and Public Works, Athens (in Greek)
[27] FEMA (2000) FEMA 356: prestandard and commentary for the seismic rehabilitation of buildings American society of civil engineers. Federal Emergency Management Agency, Washington
[28] Hanson N (1960) Precast-prestressed concrete bridges. Horizontal shear connections. Journal of the PCA Research and Development Laboratories, 2 (2):8-58
[29] Kotsira E, Dritsos S, Pilakoutas K (1993) Effectiveness of techniques for flexural repair and strengthening of RC members. Proceedings of the 5th International Conference on Structural Faults and Repair, Edinburgh, 235-243
[30] Lampropoulos A, Dritsos S (2008) Numerical study of the effects of preloading axial loading and concrete shrinkage on reinforced concrete elements strengthened by concrete layers and jackets. Seismic Engineering Conference commemorating the 1908 Messina and Reggio Calabria Earthquake, Messina, 1203-1210
[31] Loov ER Patnaik KA (1994) Horizontal shear strength of composite concrete beams with a rough interface. PSI Journal, 48-69
[32] Mast RF (1968) Auxiliary reinforcement in concrete connections. Journal of the Structural Division, Proceedings of the ASCE, 94:1485-1504
[33] Mattock AH (1976) Shear transfer under monotonic loading, across an interface between concrete cast at different times. Technical Report, Department of Civil Engineering , University of Washington, Report SM 76-3
[34] Pauley T, Park R, Phillips MH (1974) Horizontal construction joints in cast-in-plane reinforced concrete. Special Publication SP-42, ACI, Shear in Reinforced Concrete, 2:599-616
[35] PCI (1992) Design Handbook-Precast and Prestressed Concrete. Precast/Prestressed Concrete Institute, Chicago
[36] SABS 0100-1 (1992) The structural use of concrete. Council of the South African Bureau of Standards, Pretoria
[37] Saemann J, Washa G (1964) Horizontal shear connections between precast beams and cast-in-place slabs. Journal of the American Concrete Institute, 61-69:1383-1409
[38] Saidi M, Vrontinos S, Douglas B (1990) Model for the response of reinforced concrete beams strengthened by concrete overlays. ACI Structural Journal, 87:687-695
[39] Shaikh FA (1978) Proposed revisions to shear-friction provisions. PCI Journal, 23 (2):12-21
[40] Silfwerbrand J (1997) Stresses and strains in composite concrete beams subjected to differential shrinkage. ACI Structural Journal, 94(4):347-351

[41] Silfwerbrand J (1990) Improving concrete bond in repaired bridge decks. Concrete International, 36(6):419-424
[42] Silfwerbrand J (2003) Shear bond strength in repaired concrete structures. Materials and Structures, 36(6):419-424
[43] Tassios T (1983) Physical and mathematical models for redesign of repaired structures. Proceedings of the IABSE Symposium, Introductory Report, Venice
[44]Thermou G, Pantazopoulou M, Elnashai F (2007) Flexural behavior of brittle RC members rehabilitated with concrete jacketing. Journal of Structural Engineering, ASCE, 133 (10):1373-1384. doi:10.1061/(ASCE)0733-9445(2007)133:10(1373)
[45] Trikha D, Jain S, Hali S (1991) Repair and strengthening of damaged concrete beams. Concrete International: Design and Construction, 13(6):53-59
[46] Tsoukantas S and Tassios T (1989) Shear Resistance of connections between reinforced concrete linear precast elements, ACI Structural Journal, 86(3):242-249.
[47] Vassiliou G (1975) An investigation of the behaviour of repaired RC elements subjected to bending. PhD Thesis, Department of Civil Engineering, National Technical University of Athens (in Greek)
[48] Vintzeleou E (1984) Load transfer mechanisms along reinforced concrete interfaces under monotonic and cyclic actions. PhD Thesis, Department of Civil Engineering, National Technical University of Athens (in Greek)
[49] Vrontinos S, Saiidi M, Douglas B (1989) A simple model to predict the ultimate response of R/C beams with concrete overlays. Report to the National Science Foundation Research Grant CEE-8317139. Department of Civil Engineering, University of Nevada, Reno
[50] Xu R. and Wu Y. (2007) Two dimensional analytical solutions of simply supported composite beams with interlayer slips. International Journal of Solids Structures, 44:165-175. doi:10.1016/j.ijsolstr.2006.04.027
[51] Yuan Y, Li G, Cai Y (2003) Modeling for prediction of restrained shrinkage effect in concrete repair. Cement Concrete Research, 33:347-352. doi:10.1016/S0008-8846(02)00960-2
[52] Yuan Y, Marsszeky M (1994) Restrained shrinkage in repaired reinforced concrete elements. Material Structures, 27:375-382
[53] Zervos N, Beldekas V (1995) An experimental investigation on strengthening of RC beams by additional RC overlays. Dissertation Thesis, Department of Civil Engineering, University of Patras (in Greek)
[54] Zhou J, Ye G, Schlangen E, Van Breugel K (2008) Modelling of stresses and strains in bonded concrete overlays subjected to differential volume changes. Theoretical and Applied Fracture Mechanics, 49:199-205. doi:10.1016/j.tafmec.2007.11.006

## List of figures

# APPENDIX A

## Approximation of the interface shear stress distribution

In the absence of any experimental verification, several numerical analyses using ATENA finite element software (ATENA 2005) have been performed in order to define the type of shear stress distribution function along the interface. It was found that the shear stress distribution along the interface can be assumed as a cubic function of distance x. In the following, the results of one of these analyses is presented.

A simply supported concrete beam strengthened with a new concrete layer on the tensile side (Fig. 18), has been analysed using ATENA (2005) software. Details concerning ATENA modelling are presented in section 8.2 above. Specific contact elements were used in this analysis to simulate the interface behaviour, with specific values for the coefficients of friction and adhesion.

The cross sectional dimensions of the initial beam were 250 mm by 400 mm and the span length was 5000 mm. The longitudinal tensile reinforcement was four 12 mm diameter steel bars of 500 MPa yield strength and the concrete cover was 40 mm. The thickness of the additional layer was 100 mm and the additional reinforcement was two 14 mm diameter steel bars of 500 MPa yield strength, also with a concrete cover of 40 mm. The concrete strength of the beam was considered to equal 16.0 MPa something very common for old structures which need strengthening. A concentrated load was applied at mid span.

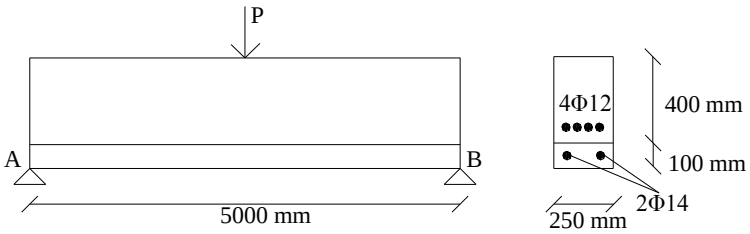


**Fig. 18** - Geometry and load condition for the beam strengthened with concrete layer on the tensile side

In Table 1, information about the concrete strength of the new layer and the interface, of the two specimens have been examined, is given.

**Table 1** Analyzed specimens

| Name of specimen | Concrete layer strength | Interface |
|---|---|---|
| S1 | 16 MPa | $\mu = 0.5$ c = 0.5 |
| S2 | 25 MPa | $\mu = 0.9$ c = 1 |

Taking into account the slip distribution derived from ATENA analysis and using Eq. (1a), the shear stress distribution along the interface of the strengthened beam can obtained, as shown in Fig. 19, together with the fitted curve described by the following equation:

$$\tau_x = A1 \cdot x^3 + B1 \tag{43}$$

where $A1$ = -0.043 and $B1$ = 0.67 for specimen S1, and $A1$ = -0,042 and $B1$ = 0.66 for specimen S2.

Therefore, in the present study, the interface shear stress distribution according to the general form of Eq. (43) has been adopted.

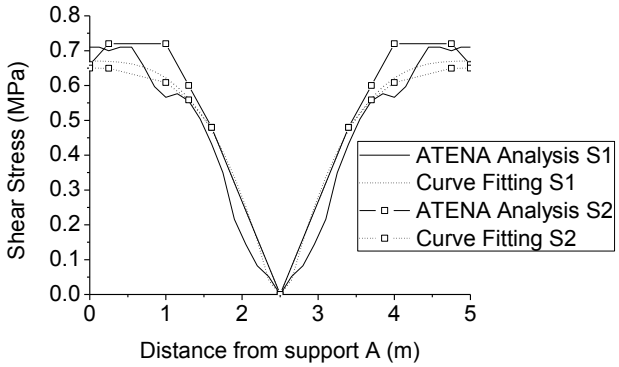


**Fig. 19** – Shear stress distribution along the interface of the strengthened beam